JOURNAL OF PROPULSION AND POWER
Vol. 12, No. 1, January–February 1996

Numerical Analysis of Sweep Effects in Shrouded Propfan Rotors

K. Helming*
DLR, German Aerospace Research Establishment, Linder Höhe, D-51140 Köln, Germany

To study blade sweep effects on loss production and energy transfer a numerical analysis has been undertaken on three 10-bladed fan rotors with low-pressure ratio and different sweep. Pressure ratio and sweep are in the typical range of propfans. The results of two rotors with 30-deg forward- and backward-swept blades are compared to those of an unswept propfan rotor. The geometry of the profiles of the swept rotors on each cylindrical position is identical with that of the unswept rotor. The numerical analysis shows that the total pressure ratio of the swept rotors is lower than that of the unswept rotor over the whole span. Only in the vicinity of the hub is the pressure ratio higher in the case of the forward-swept rotor. The decrease of the total pressure ratio at midspan, by sweeping the rotor, is due to an oblique shock with lower preshock Mach number and an increase of the boundary layer at the suction side. Sweeping the rotor has the effect to induce strong radial pressure gradients at the leading edge. The deflection of the flow towards and off the end-walls due to this pressure gradient has the effect of a changed diffusion and expansion of the flow in the vicinity of the end-walls. The emphasis of this article is not to directly provide rotors with better pressure ratios and efficiencies, but to explain the basic effects by sweeping fan-rotors as references for improving the rotor–aerodynamic.

Nomenclature

c = absolute flow velocity
h = relative blade height
M = Mach number
s = circumferential distance
u = circumferential blade velocity
α = absolute tangential flow angle
β = relative tangential flow angle
γ = meridian flow angle
Δ = difference
η = efficiency
π = pressure ratio

Subscripts
is = isentropic
rel = relative
s = swept
t = total
tan = tangential direction
u = unswept

Introduction

SWEPT blades are applied to transonic propfans and axial compressors to achieve good aerodynamic efficiency, among other reasons. Total pressure measurements have often indicated that good aerodynamic efficiency was accompanied by less total pressure rise than expected from design. One reason is that the secondary flow and shock structure have been changed by sweeping the blades.

Several investigations have been undertaken in linear cascades.[1,2] A comparison of swept and unswept rotors with cascade tests was carried out by Godwin.[3] A theoretical analysis of the flow through swept blade rows have been done by Smith and Yeh[4] and Lewis and Hill.[5] Investigations have also been undertaken in rotating swept blade rows.[6–10] The main results of these investigations can be summarized. Sweeping the blades could improve the efficiency, whereby a decrease in total pressure rise can be observed. Thereby, in the vicinity of the hub and casing, an acute angle between the blade leading edge and end-wall results in a decrease of the efficiency and an obtuse angle results in an increase of the efficiency. However, up to now the question cannot be clearly answered how sweep influences secondary flow and shock structure in a rotating transonic compressor rotor.

The subject of this investigation is a numerical analysis in order to find the reasons for these sweep effects. This is carried out on an unswept propfan rotor and two swept propfan rotors. The numerical analysis is conducted with a three-dimensional Navier–Stokes code developed by Dawes,[11] which is validated for this case by a comparison with experimental data of a ducted propfan rotor as described by Helming.[12] The special analysis is conducted by considering streamlines near suction side at 5, 50, and 95% relative blade height.

Propfan Rotors

For the numerical study a propfan rotor has been designed with a simple geometry. A sketch of the unswept and two swept rotors is shown in Fig. 1. The propfan rotor has 10 blades aligned at the leading edge. The tip diameter is 636 mm and the hub-to-tip ratio is 0.5 in order to minimize blockage effects in the hub region. The AR is 1.77. The shape of the cylindrical profiles is described by second-order equations for the pressure side and third-order equations for the suction side. The maximum blade thickness is at 50% chord length. The blades have a rounded leading edge and an acute trailing edge.

For minimizing the influence of radial work distribution a free-vortex design concept is chosen. The hub and casing shape are slightly contoured inside the blade section to avoid severe flow separation. The relative inlet Mach number is subsonic over the whole span. The camber of the suction side is shaped in such a way that a local supersonic region is established on the suction side of the rotor without sweep nearly over the whole span. The overall pressure ratio is about 1.08 with a mass flow of 48.80 kg/s and a rotor speed of 6200 rpm.

Presented as Paper 94-2695 at the AIAA/ASME/SAE/ASEE 30th Joint Propulsion Conference and Exhibit, Indianapolis, IN, June 27–29, 1994; received July 13, 1994; revision received Jan. 22, 1995; accepted for publication Jan. 31, 1995.

*Research Engineer, Institute for Propulsion Technology; currently at BMW Rolls–Royce, Aeroengines, Eschenweg 11, 15827 Dahlewitz, Germany. Member AIAA.

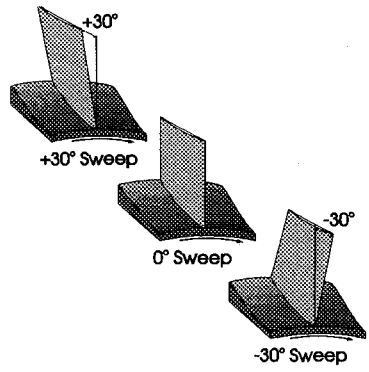

Fig. 1 Swept and unswept rotors.

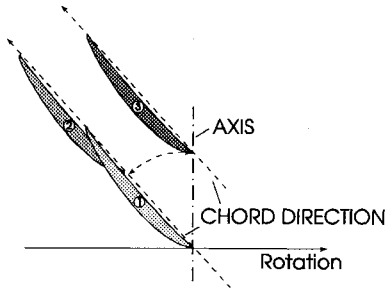

Fig. 2 Sketch of sweeping the blades.

The unswept rotor is compared with −30-deg forward- and +30-deg backward-swept rotors. The rotors are swept by shifting the blade sections in the chord direction (Fig. 2, from blade 1 to blade 2). Further, the blade sections are turned back to one circumferential position to avoid dihedral effects (Fig. 2, from blade 2 to blade 3). The contour of the casing is shifted in the axial direction in the same manner as the blades. The swept rotors are calculated for comparison with the same mass flow and rotor speed as the reference rotor.

Grid of Three-Dimensional Calculation

The numerical analysis is conducted with a three-dimensional Navier–Stokes code developed by Dawes.[11] The generated H-grid consists of 49 nodes in the blade-to-blade direction, 97 nodes in the streamwise direction, and 49 nodes in the spanwise direction. The cells are equally distributed so that one-third of the cells are located in front of, inside, and behind the blade area. The used H-grid is similar to that used for the calculation of a propfan rotor model and the results are validated with experimental data.[12] The similarity of the investigated propfan rotors to the experimentally investigated rotor should give some confidence in this numerical analysis.

The propfan rotors are calculated with tip clearance that is constant with 1.1% of tip chord length or 0.625% relative blade height. The tip clearance is modeled with three cells in the spanwise directions. The shortest distance of two neighboring nodes at the surfaces in radial direction is about 0.20% relative blade height and in the circumferential direction it is about 0.14% of the blade passage.

Analysis of Sweep Effects

The analysis starts with the description of the radial distributions of relative total pressure ratio and isentropic efficiency at the trailing edge as an overview of general effects. The observed effects of sweep will be explained by relative Mach number contours and in detail by comparing streamline values of the swept rotors with the unswept rotor. The analysis is focused on streamlines near the suction side at midspan and in the vicinity of the hub and casing.

Radial Distributions

Total Pressure Ratio and Isentropic Efficiency

The radial distribution of the relative total pressure ratio of the swept rotors are shown in Fig. 3. The change in relative total pressure ratio and difference of isentropic efficiency are defined as follows:

$$\Delta\pi_t = \frac{\pi_{t/s} - \pi_{t/u}}{\pi_{t/u} - 1}$$

$$\Delta\eta_{is} = \eta_{is/s} - \eta_{is/u}$$

It can be seen that the total pressure ratios of the swept rotors are lower than that of the unswept rotor over nearly the whole span due to a lower shock strength and increased boundary-layer thickness. In the hub region of the backward-swept rotor the flow condition has improved because the flow at the suction side is deflected more to the hub, which will be pointed out by streamlines later. Therefore, the axial velocity density ratio is higher than in the unswept case in the vicinity of the suction side and the flow turning has increased locally. The forward-swept rotor provides a very low total pressure ratio at the hub because the diffusion has increased due to the flow that is deflected more off the hub. At midspan the relative total pressure ratios are about 8–9% lower than that of the reference rotor for both rotors with sweep. An increase of the total pressure ratio can be seen in the case of the forward-swept rotor at the casing. Here, the flow is deflected to the casing at the suction side and the axial velocity density ratio becomes higher than in the unswept case, and therefore, the flow turning locally too. However, the total pressure ratio remains lower than that of the reference rotor because the local supersonic region has disappeared. The observed peak at the casing can be explained by different radial extensions of high-loss regions. The backward-swept rotor provides a very low total pressure ratio up from 80% relative blade height. Here, the shock strength has increased and provides with the streamlines (which are turned off the casing), a greater diffusion area with less flow turning. To increase the average total pressure ratio of both rotors with sweep, a redesign of the blading is necessary. However, to study basic sweep effects a redesign is not imperative.

The radial distributions of the relative isentropic efficiency of the rotors with sweep are shown in Fig. 4. The curves are

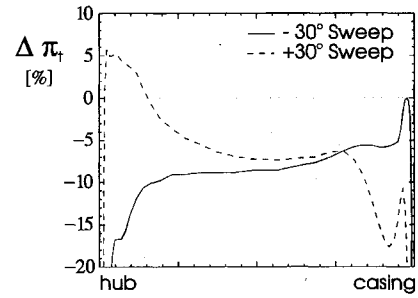

Fig. 3 Radial distribution of the relative total pressure ratio.

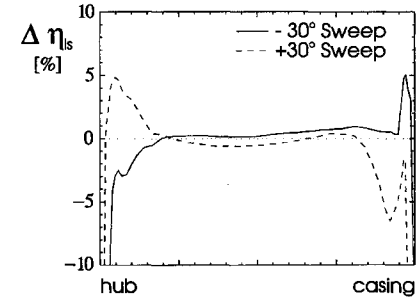

Fig. 4 Radial distribution of the difference of isentropic efficiency.

similar to those of the relative total pressure ratio. In the case of the backward-swept rotor, the efficiency is better than that of the unswept rotor in the hub region and vice versa in the case of the forward-swept rotor. At midspan the efficiencies have only small differences to that of the unswept rotor. At the casing the efficiency of the backward-swept rotor decreases severely.

The relative changes of the mass-averaged overall total pressure ratios and isentropic efficiencies as defined here are listed in Table 1.

Tangential Velocity and Relative Flow Angle

The differences of the tangential velocity ΔC_{tan} and relative flow angle $\Delta\beta$ are defined as the difference of the isentropic efficiency. Because the tangential velocity and relative flow angle become negative inside the rotor passage, the differences are positive, if the velocities and angles of the swept rotors are less than those of the reference rotor. The radial distributions of ΔC_{tan} at the trailing edge (Fig. 5) show a decrease over the whole span for both swept rotors. The radial distributions of the relative flow angle (Fig. 6) have a similar behavior as those of the tangential velocity. The angles at the trailing edge can be also interpreted as flow turning angles, because the relative flow angles in front of the rotors are identical for all three cases. Therefore, the positive differences indicate a decrease of flow turning.

The general decrease of tangential velocity and flow turning over the whole span confirm the distribution of the relative total pressure ratio, except in the vicinity of the hub of the backward-swept rotor. The higher total pressure ratio can be explained by a better isentropic efficiency due to reduced loss regions at the suction side. The mean reasons for the decrease in flow turning and tangential velocity can be given by a decreased local supersonic region with an oblique shock and an increased boundary-layer thickness, which will be shown in the following.

Table 1 Changes of overall pressure ratios and efficiencies

	−30 deg	+30 deg
$\Delta\pi_{t,ges}$, %	−8.0	−5.7
$\Delta\eta_{is,ges}$, %	−0.1	−0.6

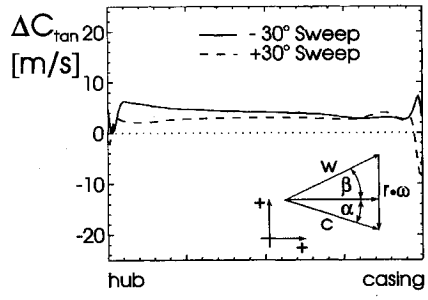

Fig. 5 Radial distribution of the difference of tangential velocity.

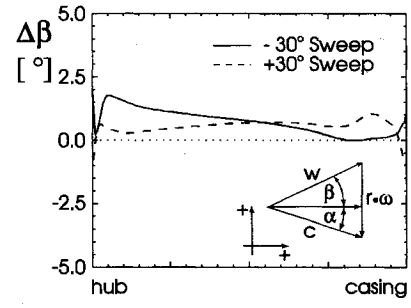

Fig. 6 Radial distribution of the difference of relative flow angle.

Relative Mach Number Contours

A first explanation for the differences of the total pressure ratio and isentropic efficiency between unswept and swept rotors can be given by looking at relative Mach number contours in the meridional plane and blade-to-blade plane.

Figure 7 shows relative Mach number contours of the blades with and without sweep in a meridional plane at 5% pitch from the suction side. Figure 7a shows the contours of the unswept rotor. The supersonic region with a preshock Mach number of about 1.20 extends over more than 50% relative blade height, whereby the shock is slightly oblique in the radial direction. With sweeping the blades 30 deg forward

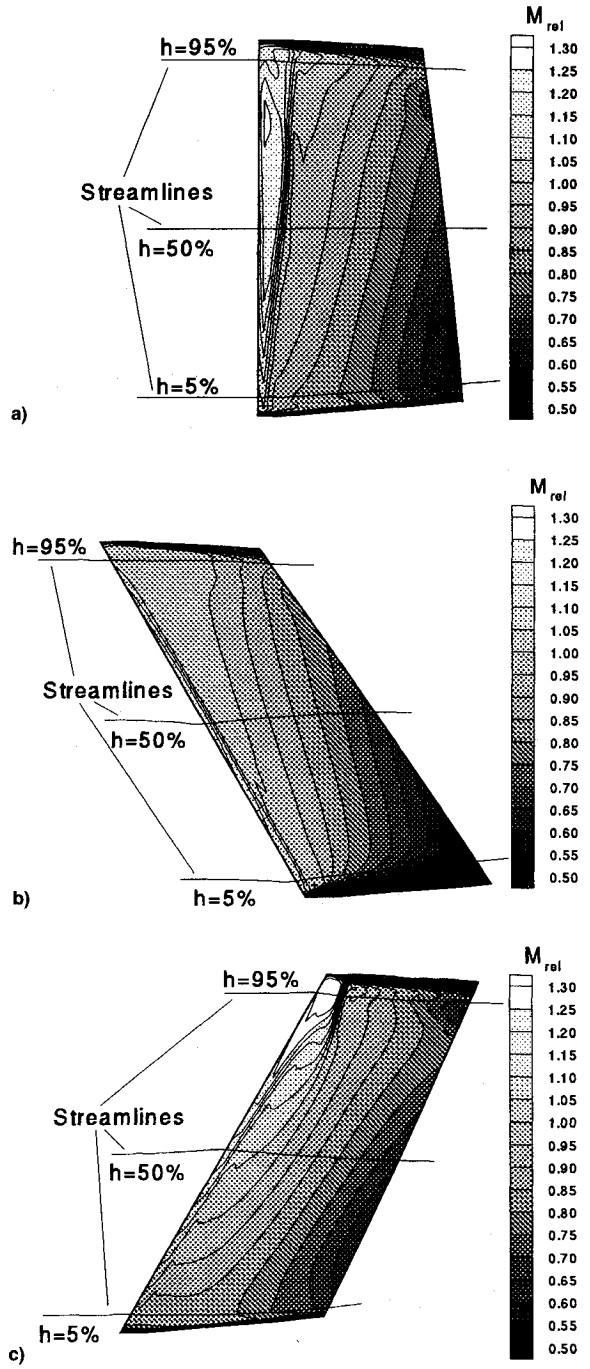

Fig. 7 Relative Mach number contours in a meridian view at 5% pitch from the suction side: a) unswept, b) forward-swept, and c) backward-swept rotors.

(Fig. 7b), the supersonic region has nearly disappeared over the whole span. At midspan the small supersonic region has an oblique shock parallel to the leading edge. In the vicinity of the casing the flow does not reach supersonic speed. A great diffusion area exists at the hub that starts at the leading edge and indicates flow separation.

In the case of the 30-deg backward-swept rotor (Fig. 7c) the supersonic region at midspan also has nearly disappeared. Opposite to the forward-swept rotor a shock still exists at the casing with a higher preshock Mach number than in the unswept case. At the hub the flow is subsonic and shows no diffusion region outside the boundary layer.

For the midspan passage the relative Mach number contours are plotted in Fig. 8. The axial and circumferential extensions of the local supersonic region can clearly be seen on the suction side for all three rotors. An extended supersonic region can be detected in the case of the unswept rotor (Fig. 8a) contrary to the swept blades (Figs. 8b and 8c). The Mach number contours of both swept blades are very similar.

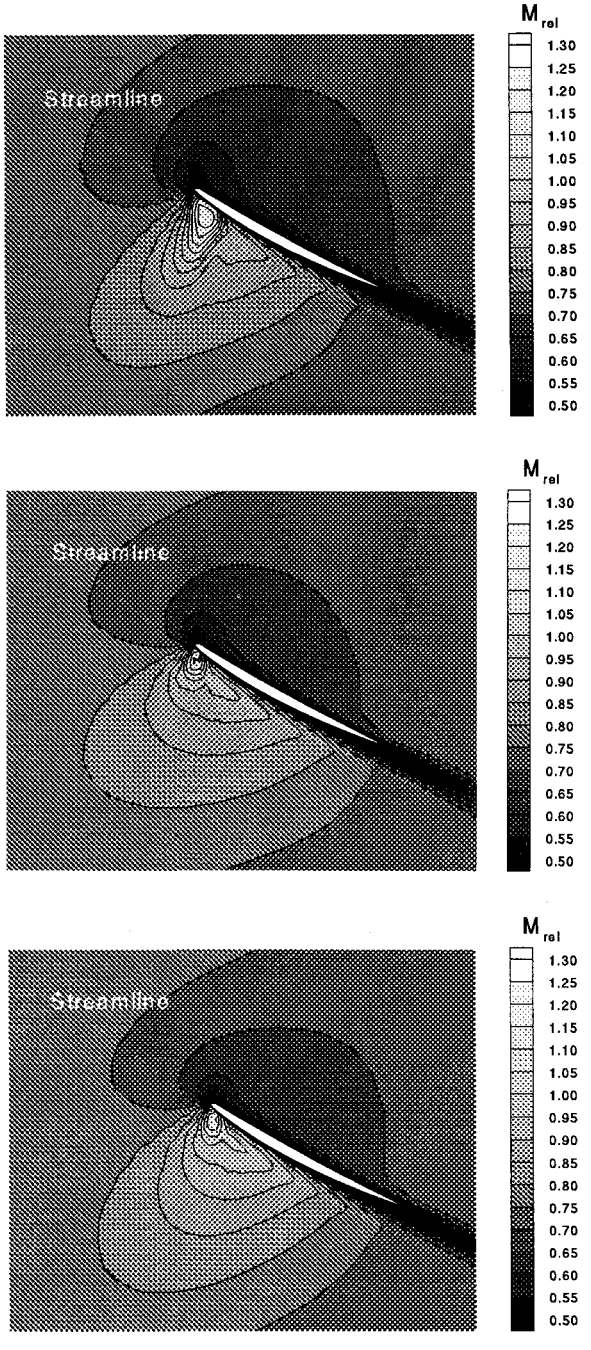

Fig. 8 Relative Mach number contours at h = 50%: a) unswept, b) forward-swept, and c) backward-swept rotors.

The Mach number contours give an overview of the global effect by sweeping the blades. It can be said that the differences in total pressure ratio and efficiency are an effect of changed local supersonic regions.

Streamlines

Streamlines are calculated at 5, 50, and 95% relative blade height in all three rotors as shown in Fig. 7. Each streamline starts at 60% relative chord length ahead of the blade and passes the leading edge at about 5% pitch from the leading edge (Fig. 8). Aerodynamic flow values are interpolated along the streamlines. These flow properties are used to explain the basic effects of sweep at midspan mainly eliminating end-wall influences.

Midspan

Figure 9a shows the relative Mach number distribution along the streamlines at midspan. In front of the rotor the relative flow decelerates more slightly in the case of the swept blades than of the unswept blade. In the case of the swept blades the local supersonic region on the suction side decreases and the preshock Mach number is about 1.05. As can be seen in Figs. 7b and 7c the shock is oblique relative to the flow direction. This means that the pressure rise over the shock is much lower than the increase of pressure over a normal shock. This effect leads to the diminished supersonic region due to nearly the same back pressure of all three rotors.

Both rotors with sweep show less turning of the flow than the 0-deg rotor. One reason could be different development of the boundary-layer thicknesses in the cases with sweep. An indication of increasing boundary-layer thickness of sweep can be found in Fig. 9c. Streamlines have been started at an h of 50% in front of the rotor in such a manner that they pass the suction side leading edge in a distance Δs of about 5% relative pitch. Different distances from the suction side can be noticed at the trailing edge for the three rotors. This result points to different boundary-layer thicknesses, which can be explained by the radial way of the streamlines (Fig. 9d). The streamline of the unswept rotor nearly remains on the same blade radius until the trailing edge. The streamline of the −30-deg rotor starts at a lower radius at the leading edge and leaves the trailing edge at 52.5% relative blade height. The streamline of the +30-deg rotor shows the opposite behavior. Both streamlines of the swept rotors indicate a longer way of the particles over the suction surface, which obviously increases the boundary-layer thickness. Because of decreasing camber of the profiles with increasing blade height, particles along the streamline of the −30-deg rotor enter a region of less diffusion than those of the rotor with backward sweep. This explains the greater boundary-layer thickness at backward sweep than at forward sweep.

Another interesting point is the flow behavior in front and in the vicinity of the leading edge near the suction side. The angle γ along the streamline of the unswept rotor remains nearly zero (Fig. 9e). Because of the weak oblique shock the flow is deflected towards the casing, as can be seen in Figs. 9d and 9e. The calculated radial pressure gradient along the streamline (Fig. 9f) shows a negative gradient at the position of the shock and proves this behavior.

Sweep has an upstream effect on the inlet flow in such a way that forward sweep deflects the flow into the direction of the hub and the backward sweep vice versa (Figs. 9d and 9e). This behavior changes completely near the leading edge. Because of the great acceleration around the nose of the profile a strong radial pressure gradient occurs (Fig. 9f). The rotor with −30-deg sweep has a positive pressure gradient upstream of the blades. This gradient suddenly changes to negative in the vicinity of the leading edge. This causes a flow turning, which is directed towards the casing. Just behind the leading

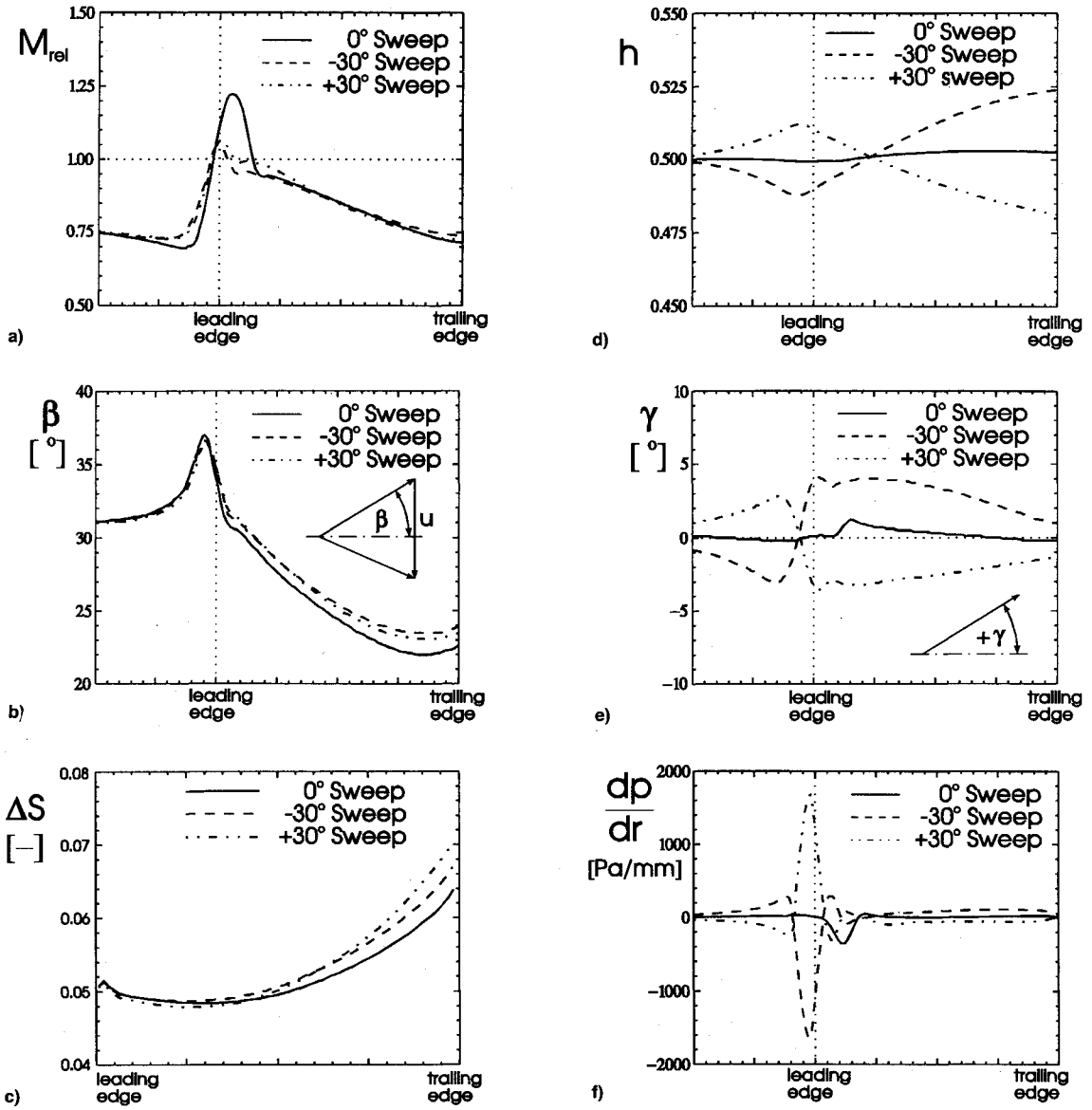

Fig. 9 a) Relative Mach number along streamlines at midspan, about 5% pitch from the suction side; b) relative flow angle along streamlines at midspan, about 5% pitch from the suction side; c) circumferential distances of the streamlines from the suction side in relation to the pitch of the leading edge, at midspan; d) relative blade height of the streamlines at midspan; e) meridian angles along streamlines at midspan, about 5% pitch from the suction side; and f) radial static pressure gradient along streamlines at midspan, about 5% pitch from the suction side.

edge the radial pressure gradient is around zero and remains nearly constant along the streamline over the blade suction surface. For this reason the flow continues towards the casing (Fig. 9d). The flow behavior of the backward-swept rotor is just the opposite.

Hub Region

As at midspan, streamlines have been started at 5% relative blade height and at a circumferential position in such a manner that they pass the suction side leading edge in a distance of about 5% relative pitch. Looking at the relative Mach number distribution of these streamlines, a high subsonic acceleration can be noticed in the entrance region of the 0- and −30-deg rotors. In contrast, the backward-swept rotor shows a typical subsonic Mach number distribution at about zero incidence.

The flow angles β (Fig. 10b) indicate increasing incidence of about 2.5 deg from backward sweep up to forward sweep. This change in incidence cannot be the only reason for the different Mach number distributions at the inlet of the blades. The radial way of the streamlines (Fig. 10c) shows the same behavior as that at midspan. If the flow is nearly axis parallel (0-deg sweep) or directed towards the hub (−30-deg sweep), a stream-tube contraction occurs because of the contoured hub. This leads to an acceleration in the entrance region. At +30-deg sweep the streamline is casing oriented and causes a moderate increase in relative Mach number.

As explained at midspan, strong radial pressure gradients occur in the vicinity of the leading edge. They change their sign from negative to positive sweep and induce an alteration of the flow angle in the radial direction. This effect can clearly be seen in Fig. 10c. The increasing diameter of the hub with increasing axial distance from the leading edge reinforces the casing-oriented flow direction at −30-deg sweep and diminishes the hub-oriented flow direction at +30-deg sweep. The latter effect leads to a moderate diffusion on the suction side (Fig. 10a) and prevents a large increase in boundary-layer thickness (Fig. 10d). The pitch related distance Δs of the streamline from the suction side nearly remains constant for the backward-swept rotor.

The other streamlines show an increasing distance from the suction side; this indicates a stronger growth of the boundary-layer thicknesses; there are two reasons for this increase. One

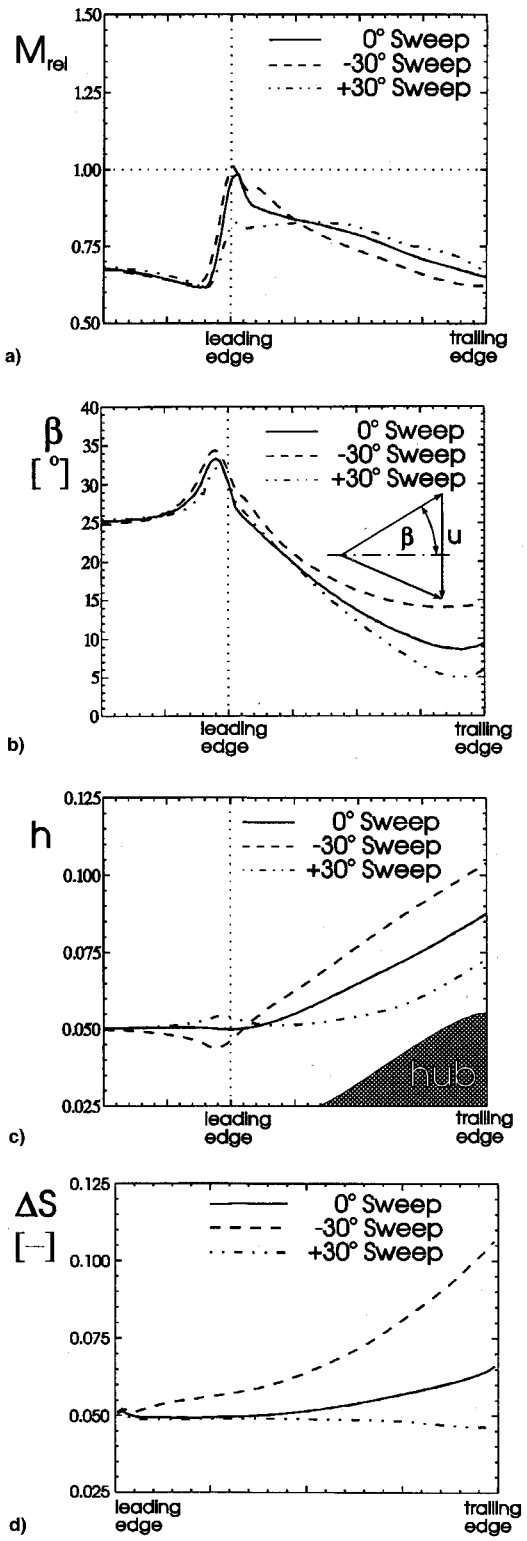

Fig. 10 a) Relative Mach number along streamlines near the hub, about 5% pitch from the suction side; b) relative flow angle along streamlines at midspan, about 5% pitch from the suction side; c) relative blade height of the streamlines near the hub; and d) circumferential distances of the streamlines from the suction side in relation to the pitch of the leading edge, near the hub.

reason is the greater diffusion due to the higher Mach number level at the beginning of the suction side of the 0- and −30-deg rotors (Fig. 10a). Further, the radial pressure gradient increases along the streamlines with increasing radius and this leads to an additional increment in diffusion. This thicker boundary layer explains the decreased turning of the flow at forward sweep, less than at backward and no sweep (Fig. 10b).

Casing

The study of the influences of sweep in the casing region is very difficult due to additional phenomena originating from tip clearance flow. The tip clearance vortex influences the flow behavior near the suction side over a great radial range, especially in the rear part of the blading. For that reason, sweep effects are studied in the entrance region of the rotors. Figure 11a shows the relative Mach number distribution along streamlines, which have been started upstream of the rotors at 95% relative blade height. The streamlines pass the suction side leading edge in a distance of about 5% relative pitch. Varying the sweep from −30 deg up to +30 deg the maximum Mach number on the suction side increases from about 0.95 to 1.35.

In the case of the forward-swept blades the flow tends towards the hub due to the upstream influence of the blades, as described previously. In contrast to the forward-sweep effect at midspan a negative radial pressure gradient cannot be built up at a low distance to the casing. This prevents a strong acceleration to high Mach numbers on the suction side in the vicinity of the leading edge. On the suction side the flow decelerates moderately and nearly follows the contour of the casing (Fig. 11b).

At +30-deg sweep the flow upstream of the rotor tends towards the casing and changes its radial direction to the hub near the leading edge (Fig. 11b). This effect occurs due to the positive radial pressure gradient in the inlet plane and is strengthened by the contoured casing. As already explained, this leads to a strong acceleration to supersonic Mach numbers. In this backward-swept case the results of the calculation show a large separation region in the vicinity of the casing on the suction surface. Up to now, it is not clear whether the separation is caused by the strong diffusion on the blade surface (Fig. 11a) or induced by tip clearance flow. To diminish

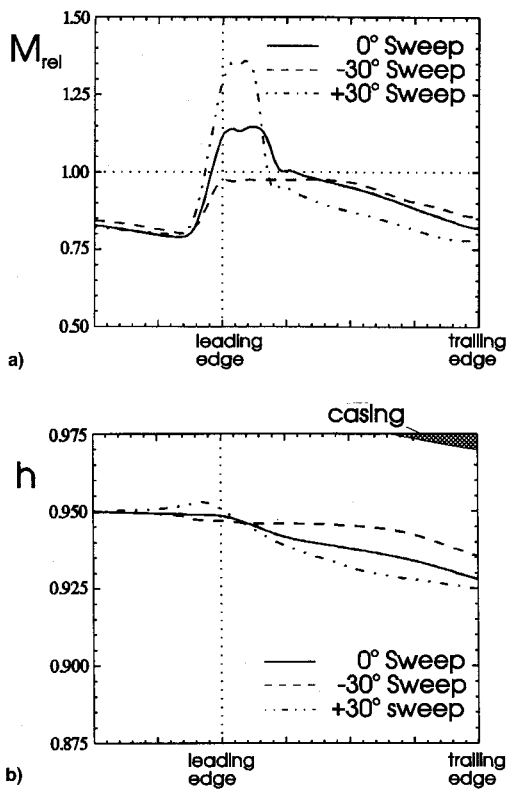

Fig. 11 a) Relative Mach number along streamlines near the casing, about 5% pitch from the suction side and b) relative blade height of the streamlines near the casing.

losses in the casing region forward sweep seems to be one good solution.

Conclusions

With a view to a better physical understanding of sweep effects on energy transfer and loss production a numerical analysis has been undertaken at transonic rotors with and without sweep. The 10-bladed rotors have low total pressure ratios, which are typical for propfans. The −30-deg forward- and +30-deg backward-swept rotors have been designed by shifting the profiles of the unswept rotor of each radius in the sweep direction. The analysis has been concentrated on sweep effects at midspan, near hub, and tip.

The flow behavior in the swept rotors is mainly influenced by two phenomena:

1) A potential upstream influence of the swept blading leads to radial pressure gradients. Forward sweep causes a negative pressure gradient and the flow tends towards the hub; at backward sweep it is vice versa.

2) The radial pressure gradient changes its sign in the rotor inlet plane near the suction side and deflects the flow radially in the opposite direction due to the so-called "suction effect."

To minimize losses, especially in the end-wall regions at the hub and tip, one can take advantage of this flow behavior at sweep. In the midspan area, away from end-wall influences, sweep diminishes shock losses, but causes an increase of boundary-layer thickness due to greater diffusion than at zero sweep.

References

[1]Stark, U., "Strömungsuntersuchungen an Gepfeilten Verdichtergittern bei Kompressibler Unterschallströmung," DFL Bericht Nr. 67-09, Jan. 1967.

[2]Shang, E., Wang, Z. Q., and Su, J. X., "The Experimental Investigations on the Compressor Cascades with Leaned and Curved Blade," American Society of Mechanical Engineers Paper 93-GT-50, May 1993.

[3]Godwin, W. R., "Effect of Sweep on Performance of Compressor Blade Sections as Indicated by Swept Blade Rotor, Unswept Blade Rotor and Cascade Tests," NACA TN 4062, 1957.

[4]Smith, L. H., and Yeh, H., "Sweep and Dihedral Effects in Axial-Flow Turbomachinery," *Journal of Basic Engineering*, Vol. 85, 1963, pp. 407–476.

[5]Lewis, R. I., and Hill, J. M., "The Influence of Sweep and Dihedral in Turbomachinery Blade Rows," *Journal of Mechanical Engineering Science*, Vol. 13, No. 4, 1971, pp. 266–285.

[6]Mohammed, K. P., and Raj, D. P., "Investigation on Axial Flow Impellers with Forward Swept Blades," American Society of Mechanical Engineers Paper 77-FE-1, 1977.

[7]Hah, C., and Wennerstrom, A. J., "Three-Dimensional Flowfields Inside a Transonic Compressor with Swept Blades," American Society of Mechanical Engineers Paper 90-GT-359, June 1990.

[8]Neubert, R. J., Hobbs, D. E., and Weingold, H. D., "Application of Sweep to Improve the Efficiency of a Transonic Fan, Part I—Design," AIAA Paper 90-1915, July 1990.

[9]Rabe, D., Hoying, D., and Koff, S., "Application of Sweep to Improve Efficiency of a Transonic Fan: Part II. Performance and Laser Test Results," AIAA Paper 91-2544, June 1991.

[10]Yamaguchi, N., Tominaga, T., Masutani, J., and Goto, M., "Performance Improvement by Forward-Skewed Blading of Axial Fan Moving Blades," ISABE 93-7055, 1993.

[11]Dawes, W. N., "A Numerical Analysis of the Three-Dimensional Viscous Flow in a Transonic Compressor Rotor and Comparison with Experiment," American Society of Mechanical Engineers Paper 86-GT-16, June 1986.

[12]Helming, K., "Experimental and Numerical Investigation of a Shock Wave Within a Swept Shrouded Propfan Rotor," American Society of Mechanical Engineers Paper 94-GT-221, June 1994.